Science of the Total Environment 1009 (2025) 181048

Contents lists available at ScienceDirect

Science of the Total Environment

journal homepage: www.elsevier.com/locate/scitotenv

Soil-biodegradable mulch film: Distinguishing between persistent microplastics and fragments released from certified soil-biodegradable products

Patrizia Marie Schmidt [a,*], Lukas Leibig [a], Lars Meyer [a], Christian Roth [a], Patrick Bolduan [a], Glauco Battagliarin [a], Andreas Künkel [a], Sam Harrison [b], Cansu Uluseker [b], Wendel Wohlleben [a]

[a] BASF SE, Carl-Bosch-Str. 38, 67056, Ludwigshafen, Germany
[b] UK Centre for Ecology & Hydrology, Library Avenue, Bailrigg, Lancaster, LA1 4AP, UK

HIGHLIGHTS

- Fragmentation is a transient phase during mulch film biodegradation.
- >90 % of polymer carbon was mineralized into CO_2 within 270 days.
- μ-FTIR microscopy tracked fragment size and count over time.
- FRAGMENT-MNP model predicts particle decline below $1/g_{soil}$ in ~600 days.
- Cryomilled films degrade faster and fragment more than 1 cm^2 pieces.

GRAPHICAL ABSTRACT

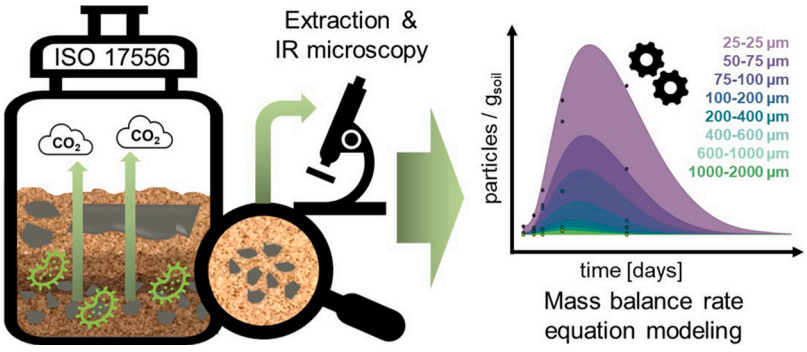

ARTICLE INFO

Keywords:
Biodegradation
Mulch film
Microplastics
Fragmentation
Persistence
Soil
Modelling

ABSTRACT

Soil-biodegradable mulch films offer a sustainable alternative to conventional plastics in agriculture, especially where recollection or recycling are impractical. However, biodegradation of these materials must not result in the formation of persistent microplastics. This study investigates the fragmentation and biodegradation of the certified soil-biodegradable mulch film ecovio® M2351 in standardized laboratory conditions (ISO 17556). The material was incubated in agricultural soil in two different forms: cryomilled fragments and 1 cm^2 film pieces. Fragment formation was quantified using μ-FTIR microscopy. Biodegradation as well as fragmentation kinetics were modelled by the open-source mechanistic FRAGMENT-MNP model. Results demonstrate that fragmentation is a transient phase within the biodegradation process, with particle counts transitionally peaking, then declining as mineralization progresses. Cryomilled fragments exhibited faster biodegradation and more pronounced fragmentation than larger film pieces. When biodegradation experiments were stopped, more than 90 % of the polymeric carbon was converted into CO_2 and residual fragments showed comparable chemical composition to the original material but showed significantly reduced molar masses, indicating that the biodegradation was still progressing. This is supported by the model, predicting that particle concentrations will decrease to below one particle per gram of soil within 600–700 days for both scenarios. These findings confirm that certified soil-

* Corresponding author.
E-mail address: patrizia-marie.schmidt@basf.com (P.M. Schmidt).

https://doi.org/10.1016/j.scitotenv.2025.181048
Received 22 September 2025; Received in revised form 4 November 2025; Accepted 21 November 2025
Available online 27 November 2025

biodegradable polymers like ecovio® M2351 do not form persistent microplastics. The combined experimental and modelling approach provides mechanistic insights into the interplay between fragmentation and mineralization and could be further improved by additional measurements of fragments <25 μm and of the polymer mass in the dissolved phase. In future, field data can support the extrapolation of the model predictions to the real-world.

1. Introduction

The agricultural sector heavily relies on plastic mulch films, which help maintain stable temperature and moisture levels while preventing weed growth, ultimately enhancing crop yields (von Vacano et al., 2022; Hofmann et al., 2023; Liu et al., 2014; Merino et al., 2019). After use, these mulch films are contaminated with soil and plant residues and partially degraded, rendering recollection and recycling technically or economically unfeasible, resulting in landfilling or incineration. Over time, especially through harsh mechanical processes (Park and Kim, 2022; Rillig et al., 2017; Li et al., 2023a) or ultraviolet (UV) aging (Zhang et al., 2024; Wang et al., 2021), fragments of these mulch films can be formed and enter into the soil, where they may persist, if not biodegradable, as secondary microplastics (Fig. 1) (ECHA, 2019). Such secondary microplastics are targeted by the upcoming Ecodesign for Sustainable Product Regulation (ESPR), aiming to find alternative, more sustainable products with reduced microplastic release (European Commission, 2024). Today, soil-biodegradable plastics are already utilized as alternative for the production of thin mulch films, typically with less than 25 μm in thickness. Unlike thin polyethylene (PE) films (Gao et al., 2021; Gu et al., 2021), certified soil-biodegradable mulch films are designed to biodegrade in the soil (Sander, 2019; Zumstein et al., 2018; Nelson et al., 2020). Therefore, fragments released by certified soil-biodegradable products should only occur transitionally during biodegradation and not accumulate (Fig. 1) as it is the case of secondary microplastics released from conventional plastics (Wohlleben et al., 2023; Pfohl et al., 2024a; Degli-Innocenti, 2024). However, it is still imperative to ensure that products based on these certified soil-biodegradable polymers can be completely mineralized into carbon dioxide (CO_2) and biomass, leaving no persistent microplastics behind. This can be done by complementing standardized biodegradation tests for certification with thorough fragment analysis used in microplastic research (Su et al., 2024; Pfohl et al., 2022; Binda et al., 2024). While standardized biodegradation tests prove the biodegradability of the material in soil (Zumstein et al., 2018; Künkel et al., 2016; Chinaglia et al., 2018; Leja and Lewandowicz, 2010), advanced microplastic extraction and analysis techniques, such as μ-Raman or μ-FTIR microscopy, can analyze residual polymer at the level of individual particles, with sizes as small as 5 μm (Araujo et al., 2018; Kappler et al., 2016).

In this study, we applied the aforementioned approach to investigate the biodegradation and fragmentation of a certified soil-biodegradable mulch film known as ecovio® M2351. To achieve this, we conducted laboratory experiments in accordance with ISO 17556 standards, employing two distinct scenarios: 1) cryomilled mulch film fragments evenly distributed within the soil, and 2) 1 cm^2 pieces arranged within soil layers. To analyze the fragments generated from the original mulch film during biodegradation, we utilized our previously validated method that involved centrifugation for fragment extraction (Pfohl et al., 2024b), followed by infrared microscopy (μ-FTIR) to assess the number, shape, size, and chemical composition of the fragments. The μ-FTIR measurements were extensively optimized in terms of particle numbers, size, contrast between particles and filter, and library and search parameters. Additionally, we measured the molar mass distribution at various time points throughout the biodegradation process to examine the polymer chain scission mechanism. The data we gathered contributed to the refinement of a mechanistic model known as FRAGMENT-MNP (Harrison et al., 2025), which enables to compare the biodegradation and fragmentation mechanisms of both large and small mulch film pieces in soil. Furthermore, this model can predict the rate at which fragments biodegrade and further decay into smaller pieces in the environment and of estimating the time required for complete disappearance of each fragment (half-life predictions). It can also estimate the peak of fragmentation for each size class. These parameters will vary depending on the type of polymer employed and the prevailing environmental conditions, highlighting the necessity for additional data to further enhance the accuracy of the model's predictions.

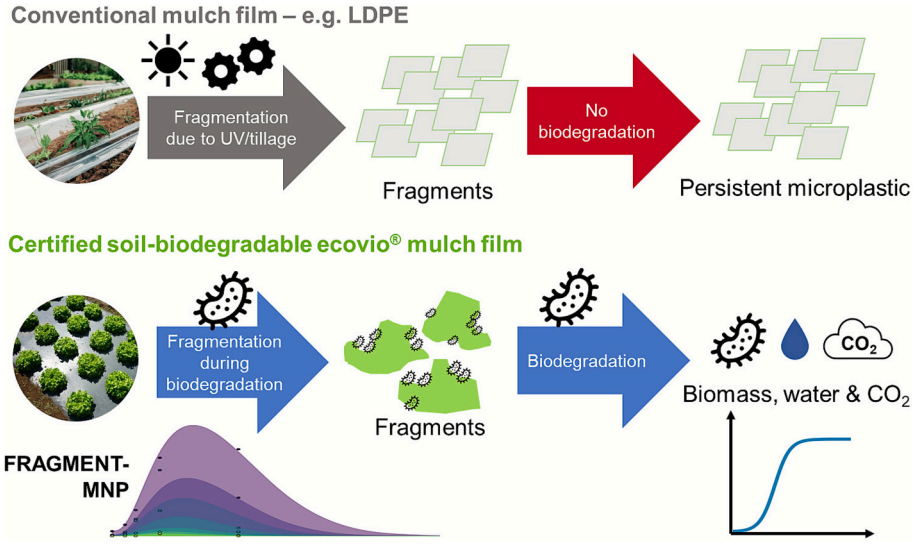

Fig. 1. Fragmentation processes of conventional vs. certified soil-biodegradable mulch films. Conventional mulch films release fragments due to UV aging or mechanical treatments which cannot be further biodegraded and will therefore remain in the soil as persistent microplastics. In contrast to that fragments from certified soil-biodegradable mulch films are already formed during the biodegradation process and will further be converted into CO_2, biomass and water. All steps of this process can be modelled with the mechanistic FRAGMENT-MNP model.

2. Materials

For the experiments, the certified soil-biodegradable ecovio® M2351 was used, a compound based on the biodegradable copolyester ecoflex® F Blend and polylactic acid (PLA) (BASF SE, 2024). Black mulch films of ecovio® M2351 with a thickness of 12 μm were cryomilled using a Retsch ZM 200 ultra-centrifugal mill and liquid nitrogen. After sieving, the fraction 100–300 μm was kept and dried in a vacuum oven at 36 °C for 48 h. In addition, 1 cm^2 pieces of the same ecovio® M2351 black mulch film were cut by hand, representing macroplastics. The material was characterized using gel permeation chromatography (GPC) to assess molar mass distribution and through elemental analysis, which measured the content of carbon (both organic and inorganic), hydrogen, and ash to quantify content of inorganic residues. Oxygen content was assumed to be the remaining mass of the material. For the biodegradation tests, microcrystalline cellulose was used as positive control, while low-density PE (LDPE) in 25 μm thickness served as negative control. The soil biodegradation tests were performed using a soil from a lysimeter from BASF Agricultural Center Limburgerhof, Germany. Characterization data and information about the mulch film and the soil can be found in Tables S1 and S2 in the Supporting Information (SI).

3. Methods

3.1. Soil-biodegradation tests

The biodegradation test was conducted using a scaled-down version of ISO 17556. Twenty-three 250 mL Duran® bottles were prepared with 50 g of dry soil mass. This included: blank soil (triplicates) for baseline activity; soil mixed with microcrystalline cellulose (105.8 mg) as a positive control (duplicates); cryomilled ecovio® M2351 powder (94.6 mg) and 1 cm^2 film pieces (94.6 mg) in soil (8 replicates each); and 1 cm^2 LDPE film pieces (53.6 mg) (duplicates). Soil was mixed with Millipore water to reach 50 % moisture. OxiTop® devices monitored pressure changes and biodegradation, while CO_2 was measured using a Shimadzu Total Organic Carbon Analyzer. Measurements were taken at various biodegradation levels. More precise information about the biodegradation experiments can be found in the SI.

3.2. Fragment extraction and analysis

Soil samples containing the test material were freeze-dried and homogenized using a Turbula®System Schatz T2F without a fixed rotating axis for 1 h. Afterwards, 2 g subsamples were taken out in duplicate. The protocol which was used to extract certified soil-biodegradable mulch film fragments from these soil subsamples has been previously published in detail (Pfohl et al., 2024b). In short, the protocol is based on a combination of sample deagglomeration and centrifugation with varying densities of a sodium polytungstate (SPT) solution. To separate the different density fractions, a novel freezing and cutting approach was used, resulting in minimal soil contamination in the final extracts. The protocol was validated in terms of microplastic recovery and matrix removal efficiency from different types of soil as well as in terms of polymer and particle stability. For the purpose of this study, recovery tests were repeated with the cryomilled fragments of ecovio® M2351 used herein, resulting in a recovery rate of 100.0 ± 2.2 wt.-%. The extracted particles were analyzed via μ-FTIR microscopy to assess the particle number, size, shape, and identity. In addition, Soxhlet extraction was performed at the endpoint of the biodegradation experiment for the cryomilled mulch film (>90 % CO_2), to analyze the molar mass of remaining fragments. Details of the μ-FTIR measurements, Soxhlet extraction and GPC are reported in the SI.

3.3. Modelling the time evolution of particle sizes

To better understand fragmentation and mineralization kinetics and thereby predict the time required for the complete disappearance of fragments, we employed the fragmentation model FRAGMENT-MNP (Harrison et al., 2025), which was further extended as part of this work to track mineralized polymer. The model, available as an open-source Python package, predicts the mass-based time evolution of binned particle size distributions, “discorporated” polymer (e.g. dissolved monomers, oligomers, biomass and volatile organic compounds) and mineralized CO_2. Rate constants govern the rates at which mass is transferred from larger to smaller size classes (k_{frag}; fragmentation rate constant), from particles to discorporated polymer (k_{diss}; dissolution/discorporation rate constant) and from discorporated to mineralized CO_2 (k_{min}; mineralization rate constant). These rate constants can be a function of time (k_{frag}, k_{diss} and k_{min}) and particle surface area (k_{frag} and k_{diss}), with the nature of this dependence able to take an arbitrary-shaped regression specified by the user. The model documentation (https://fragmentmnp.ceh.ac.uk/) provides detailed information about all aspects of using the model.

We fitted the model to measurement data by minimizing a cost function that compared the closeness of the model fit to these data. The input parameters that were allowed to vary as part of this optimization included the initial concentrations of polymer, rate constants, and parameters controlling the time- and surface-area-dependence of rate constants. Thus, the output of the optimization tells us about the rate constants that best fit measurement data, offering mechanistic insight into the underlying biodegradation processes. The optimization was implemented in a custom Python script, making use of the differential evolution algorithm followed by Nelder-Mead refinement to ensure robust parameter estimation. To ensure convergence to meaningful solutions, the optimization was performed in two stages: an initial global search using Differential Evolution to explore the parameter space broadly, followed by local refinement using the Nelder–Mead algorithm to fine-tune the best solutions.

The optimization aimed to minimize a composite cost function that quantified the deviation between model predictions and experimental observations. Three key data sources were integrated into this cost function: the temporal evolution of particle mass across size classes, the corresponding particle number concentrations, and cumulative CO_2 evolution over time as a proxy for mineralization.

Model fitting involved simulation of a population of particles distributed across defined size bins, using an ordinary differential equation (ODE) solver to integrate the system over time. To compare simulation output with experimental observations, mass predictions were converted to particle number concentrations using measured mass-per-particle values. A structured weighting scheme was applied in the cost function to emphasize particular time points and size classes. Full details, including the code used to perform the optimization, are available in the SI and Zenodo (Uluseker et al., 2025).

To ensure the reproducibility and comparability of our findings, all experimental procedures, data, and modelling approaches are described in detail and are available in the SI. The methodologies applied in this study are based on internationally recognized standards (e.g., ISO 17556) and microplastic extraction, analysis and modelling have been advanced and validated in previous research by various laboratories (Möller et al., 2022; Ruffell et al., 2024; Chen et al., 2024; Brouwer et al., 2024).

4. Results and discussion

4.1. The influence of the test set-up on the biodegradation of certified soil-biodegradable mulch film

In this study, we utilized two different shapes of ecovio® M2351 to investigate the impact on the biodegradation and fragmentation. The cryomilled powder was evenly distributed within the soil, while the 1 cm^2 film pieces were arranged in 3 layers each separated by soil layers.

Fig. S2 shows the biodegradation curves for the different materials tested until plateau. In both cases >90 % of polymeric carbon was mineralized into CO_2, confirming biodegradability. For the cryomilled fragments the process took about 180 days, for the 1 cm^2 pieces it took about 270 days, but in both cases the biodegradation was comparable (1 cm^2 pieces) to or even higher (cryomilled) than that of the cellulose positive control. In contrast to that, the LDPE negative control showed no biodegradation, staying below 0.6 % CO_2 throughout the experiment. A comparison between the mineralization curves (Fig. S3a + b) shows the influence of the biological variability on material biodegradation. Although all experiments were initiated simultaneously using the same soil and maintaining constant parameters, the curve progression reveals slight variations, particularly evident in the samples that were stopped after 60 % conversion of the polymer carbon into CO_2. Overall, the trend remains consistent: for all samples tested in powder form a more rapid mineralization could be observed compared to the 1 cm^2 films. This supports our hypothesis that the biodegradation rate depends on the film's surface area and its accessibility to microbes. Cryomilled fragments have a larger total surface area and can be more evenly dispersed in the soil than the 1 cm^2 pieces, which were placed between soil layers. Their greater accessibility to microbes explains the faster biodegradation observed. We therefore conclude that the test setup can influence the biodegradation results.

When comparing standardized laboratory tests with real-world field conditions, it is important to note that environmental variables, such as temperature, humidity, microbial diversity, and soil composition, can affect biodegradation rates. These factors can vary even between similar fields, which is why combining controlled laboratory tests with field experiments is essential for a comprehensive understanding.

4.2. Understanding the interconnected processes of biodegradation and fragmentation

After extracting remaining fragments of ecovio® M2351 from soil at the different timepoints of biodegradation, subsamples of the extracts were filtered for μ-FTIR analysis. Fig. 2 shows exemplary pictures of these filters (campaign containing cryomilled ecovio® M2351) and below close-ups of selected fragments which were identified as ecovio® M2351. Through visual inspection of these images, several qualitative observations suggest what may have happened during the biodegradation experiment: initially, large fragments are present, displaying sharp edges as a result of the cryomilling process. By the time 10 % CO_2 is reached, the particles have already diminished significantly in size, and a greater number of small fragments are visible on the filter. As polymer conversion into CO_2 continues, the visible count of fragments decreases, and so do their sizes. Close-up examinations reveal that the sharp edges gradually disappear over biodegradation time, resulting in more rounded shapes. When >90 % CO_2 conversion is reached, only a few very small fragments remain.

These visual inspections are further supported by measurement data obtained via μ-FTIR, demonstrating that fragmentation is a transient phase in the biodegradation of certified soil-biodegradable mulch films. In the case of the cryomilled fragments (Fig. 3a), the measurement data aligns closely with the visual observations noted on the filter: initially, a low total particle count of large fragments was detected at the beginning of the biodegradation experiment. However, an intense increase in total particle counts per gram soil was observed after just 18 days (10 % CO_2), attributed to the intense fragmentation of the original film pieces. This high total particle count still remained after 30 days of biodegradation (30 % CO_2) but began to decline as biodegradation progressed. After 77 days of biodegradation (60 % CO_2), the total particle count started to decrease, indicating that the previously formed fragments were further converted into CO_2 and biomass. This process of biodegradation and mineralization continued over time, demonstrating an approximate 87 % reduction in total particle counts from the peak observed at 30 days to the end of the experiment at 269 days. For the 1 cm^2 pieces (Fig. 3d), the μ-FTIR analysis focused exclusively on fragments <1 mm, while the mass of remaining fragments >1 mm was determined through manual weighing. As a result, the dataset presented in Fig. 3d began with a very low total particle count of approximately 45 counts per gram soil for fragments <1 mm. Nevertheless, also in this case, we observed an increase in total particle counts per gram soil as biodegradation progressed, attributed to the fragmentation of the 1 cm^2 mulch film pieces during the biodegradation process. The peak of total particle counts, however, occurred at a later stage in the biodegradation process compared to the cryomilled mulch film, specifically after 84 days (60 % CO_2). Similarly as before, we noted a decrease in total particle counts (of about 30 %) from this fragmentation peak until the end of the experiment at 269 days. In general, the total particle counts per gram soil detected at different timepoints in the set-up with the 1 cm^2 pieces was lower than in the set-up with the cryomilled film pieces. In addition to the samples containing ecovio® M2351, soil blanks were extracted to compare the spiked samples against any potential background contamination (Fig. S4).

Looking into the particle size distributions (Fig. S5) of ecovio® M2351 fragments detected by μ-FTIR at the different timepoints of the biodegradation experiments in both scenarios, two size classes can be highlighted: 1) The fraction of particles with sizes 100–200 μm since this was the main fraction that was formed transitionally during biodegradation of the cryomilled mulch film and 2) the fraction of particles with

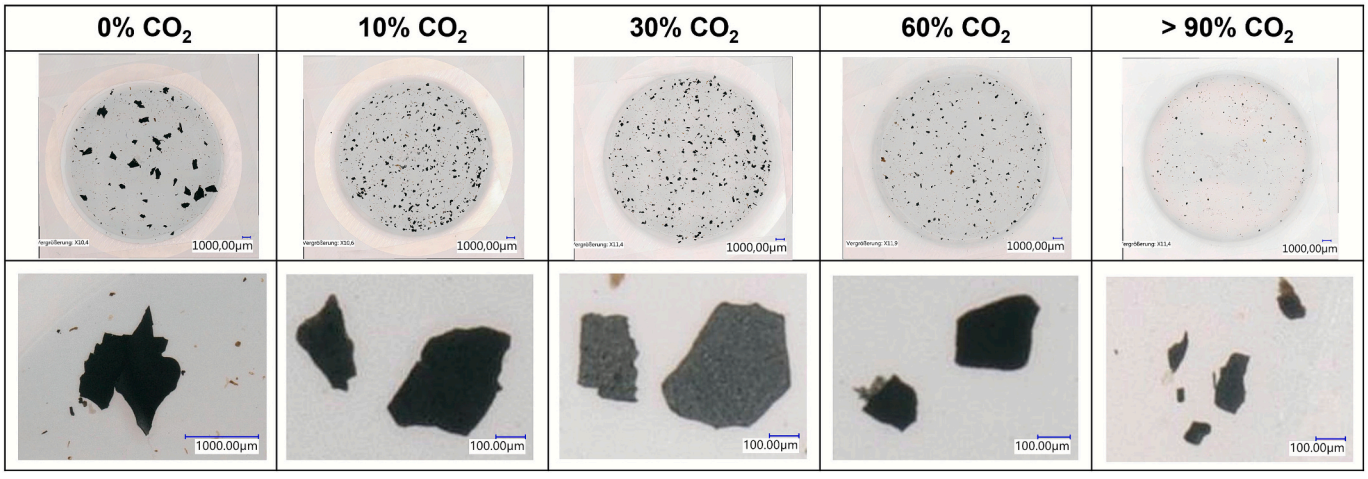

Fig. 2. Representative pictures of filters and shapes of ecovio® M2351 fragments at different timepoints after extraction from soil (test set-up with cryomilled mulch film). Particles shown exhibited the characteristic IR spectrum of ecovio® M2351.

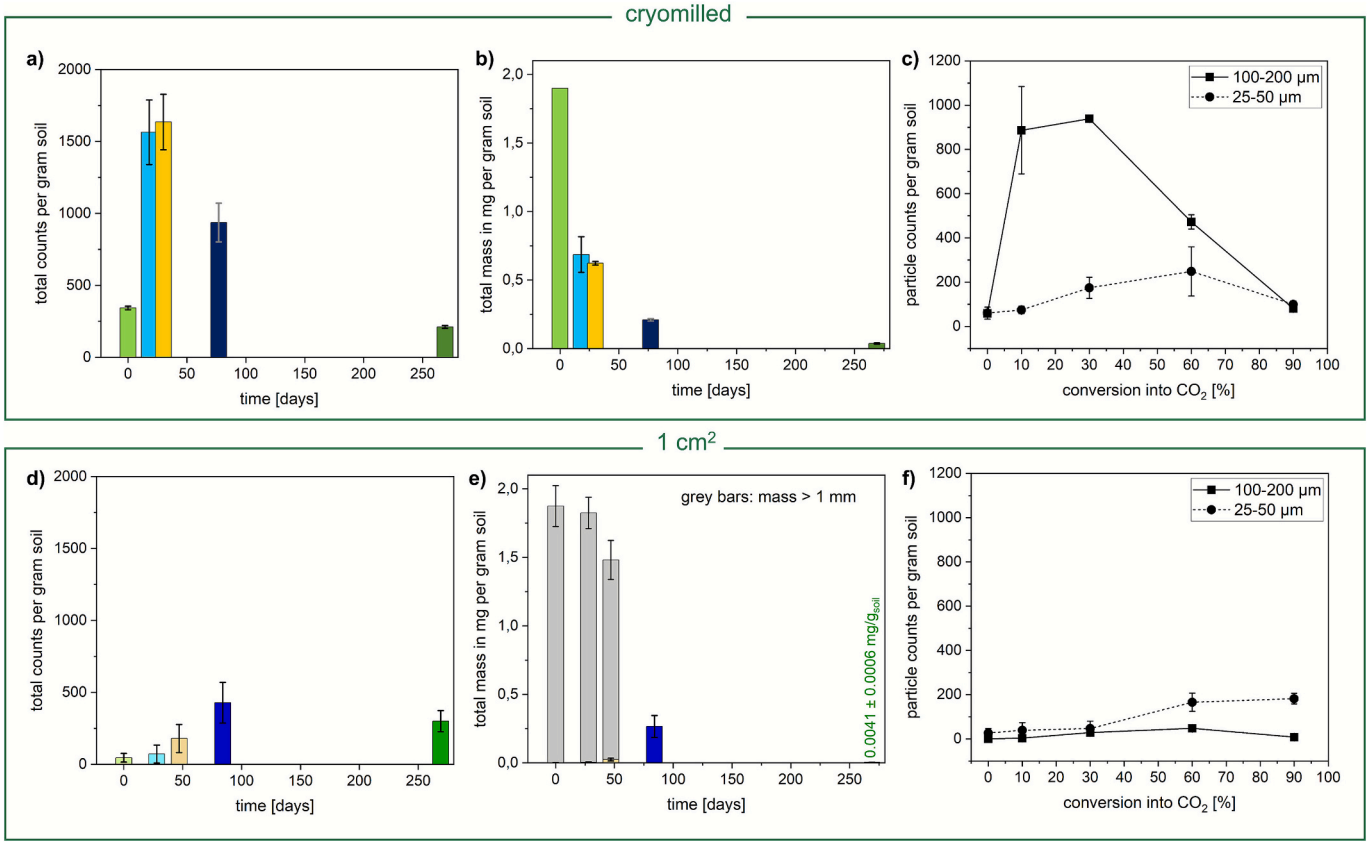

Fig. 3. Measured total particle counts <1 mm (a and d) and determined total mulch film mass (b and e) over biodegradation time for the two scenarios of cryomilled films and 1 cm^2 pieces. Evolution of fragment counts with sizes ranging from 100 to 200 µm and 25–50 µm during biodegradation of c) cryomilled and f) 1 cm^2 pieces of ecovio® M2351.

sizes 25–50 µm, since this was the main fraction formed at later timepoints of both biodegradation experiments. Fig. 3c+f shows the evolution specifically for those fractions in both scenarios over CO_2. For the cryomilled mulch film, the increase in counts for particles sized 100–200 µm is approximately 15-fold by the early stages of the biodegradation experiment (10 % CO_2). In contrast, the smaller size fraction of 25–50 µm reaches its peak later in the biodegradation process (60 % CO_2). Following their peak, the particle counts in both size fractions decline, yet they do not reach zero by the end of the conducted biodegradation experiment. In contrast to the cryomilled mulch film, in the set-up with the 1 cm^2 film pieces, the counts of fragments in the size range 25–50 µm was at all timepoints higher than the counts of fragments in the size range 100–200 µm. The total counts of the fraction 25–50 µm started to increase at 60 % CO_2 and even continued to increase until the end of the biodegradation experiment.

To estimate the evolution of polymer mass during biodegradation, and to enable fitting of the mass-based FRAGMENT-MNP model, the measured fragment counts were converted into mass by considering the particle size distributions, the density and thickness of the mulch film, and assuming a disc shape based on the equivalent circle diameter determined by µ-FTIR analysis. In addition, it was assumed that also the thickness of the fragments was reduced during biodegradation and was estimated to 25 % of the original film thickness of 15 µm at 90 % CO_2. In the case of the 1 cm^2 pieces, the mass of remaining fragments >1 mm was determined manually by weighing and was added to the mass of fragments <1 mm. The mass conversion was done for all timepoints and calculated masses are shown in Fig. 3b+e to compare fragment masses at different timepoints. When comparing the fragment number evolution with the mass evolution, it becomes evident, that even though there is first an increase in total particle counts detected due to fragmentation, biodegradation and conversion of polymer carbon into CO_2 takes place at the same time, leading to a rapid reduction of the overall polymer mass by 98.1 wt.-% from the beginning of the experiment until 90 % CO_2 is reached. Even though we found only low fragment counts <1 mm in the set-up with 1 cm^2 film pieces, the data clearly show that the main proportion of the polymer mass still was in the size fraction >1 mm before the mass was rapidly reduced when reaching 60 % CO_2 and no more fragments >1 mm were found. Fig. S6a illustrates the determined data on a logarithmic scale to provide a clearer representation of the mass evolution of fragments <1 mm. The data reveal that the mass of the fraction <1 mm initially increases as the 1 cm^2 pieces fragment into smaller particles. Subsequently, there is also a notable decrease in fragment mass by 98.5 wt.-% from 60 % CO_2 to 90 % CO_2. The overall mass was reduced by 99.8 wt.-% from the beginning until the end of the biodegradation experiment, confirming the successful biodegradation of the material.

However, at the end of the biodegradation experiment, some fragments were still detected in both scenarios: approximately 200 fragments in the case of the cryomilled mulch film and around 300 fragments resulting from the 1 cm^2 pieces. Although the particle count was higher in the latter case, the mass of these fragments differed by an order of magnitude, with the 1 cm^2 pieces exhibiting a lower mass. This discrepancy is attributed to the smaller sizes of the 300 particles compared to the 200 particles observed in the cryomilled mulch film scenario. To gain a deeper understanding of potential further biodegradation or accumulation of the remaining fragments, Soxhlet extraction and GPC analysis was used to detect changes in molar mass of the cryomilled mulch film fragments between the beginning and the end of the experiments (Fig. S7). As controls, a soil blank and the original mulch film were treated in the same way. The Soxhlet extraction induced a slight reduction of the molar mass of ecovio® M2351. Still, differences can be detected between the cryomilled ecovio® M2351

fragments before biodegradation and the ones remaining at the end of the biodegradation experiment. In line with the biodegradation curves of the material, a reduction of molar mass was observed and a second peak with low molar masses <10,000 g/mol started to evolve. This result underlines, that no persistent microplastics were formed from ecovio® M2351 during biodegradation, for which we would expect an enrichment of fragments with high molar mass, non-cleavable polymer bonds in the main chain, or crosslinked polymer (Żenkiewicz et al., 2012; Chen et al., 1997; Erlandsson et al., 1998). Instead, the molar mass reduction and the chemical similarity to the original material demonstrate that the biodegradation of the remaining fragments was still ongoing when the experiment was stopped.

In addition, the discrepancy between measured CO_2 and remaining fragment mass must be addressed. Fig. S6b + c shows the mass of ecovio® M2351 over CO_2, revealing that the remaining mass is lower than expected if all unconverted polymer were solid fragments. For cryomilled fragments, the remaining mass was about 1.9 wt.-% of the original polymer mass, while for 1 cm^2 pieces, it was approximately 0.2 wt.-%. This study analyzed particle sizes down to 25 μm due to the sieving step for μ-FTIR analysis. Therefore, we cannot exclude that missing polymer mass at the end of the biodegradation experiment may still exist as fragments <25 μm. A targeted extraction technique and subsequent analysis would be needed to quantify small micro- and nanoplastics (Schwaferts et al., 2020; Ivleva, 2021; Li et al., 2023b; Okoffo and Thomas, 2024). To assess the likelihood of this hypothesis, we analyzed the fraction <25 μm at 90 % CO_2 from the 1 cm^2 pieces. If valid, we would expect to find 0.186 mg/g_{soil} in fragments <25 μm, translating to approximately 113,000 fragments/g_{soil} at 20 μm, 1,800,000 fragments/g_{soil} at 5 μm, or 45,110,000 fragments/g_{soil} at 1 μm, or a combination of several sizes. These numbers are at least two orders of magnitude greater than the actual measured counts, which indicate approximately 3417 ± 878 particles per gram of soil within the size range of 10 to 25 μm. This discrepancy leads us to argue that the missing polymer mass is unlikely to exist as small micro- and nanoplastics. Rather, it has likely been transformed into biomass, as discussed in the literature (Zumstein et al., 2018).

4.3. Biodegradation and fragmentation modelling

In addition to experimental data, modelling can help tackle issues such as the limit of quantification of analytical techniques and extend the predictive power of experimental studies by estimating fragment stability beyond the duration of laboratory observations. It also enables the identification of key degradation milestones, such as the timing of peak fragmentation and the decline of particle concentrations below environmentally relevant thresholds. In this study, the experimental data was used to parameterize the mechanistic FRAGMENT-MNP model. Results are discussed in the following sections.

4.3.1. CO_2 mineralization fit

The ability of the model to reproduce mineralization kinetics was evaluated by comparing observed and modelled cumulative CO_2 evolution. As shown in Figs. S9 and S10, the modelled CO_2 fraction closely follows the experimental measurements for both cryomilled and 1 cm^2 mulch films. The observed CO_2 data and model prediction align well across the full duration of the experiment, suggesting that the model captures the mineralization dynamics accurately in both conditions.

4.3.2. Fit to particle number distributions

To evaluate how the model captured the size-resolved fragmentation dynamics, model-predicted and observed particle number concentrations are compared across all experimental timepoints and size bins. This comparison revealed a strong agreement between the model and the experimental data, particularly during the early biodegradation timepoints. For both the cryomilled and 1 cm^2 mulch films, the model successfully reproduced the overall distribution and temporal decline of particle numbers. At each timepoint, the particle number concentrations per size class were visualized as bar charts (model) overlapped with observed data points (dots), offering a detailed view of the model fit (Figs. S11 and S12).

In the case of cryomilled fragments, the model aligned with observations during the initial phases, capturing the rapid generation and subsequent decline of particles across size classes. However, at later timepoints, the model tended to underestimate the number of particles, particularly in the smallest size bin, suggesting potential limitations in capturing the full extent of fragmentation of small-scale particles. One explanation is that the model sums up the total polymer mass present in CO_2, dissolved material, and solid fragments in the different fragment size bins. It is currently parameterized using only CO_2 data and fragment data for 25–1000 μm because of the analytical limitations. Consequently, the model can sometimes overestimate larger particles or the polymer mass in the dissolved fraction while underestimating smaller particles, with their mass being allocated instead to a larger size bin or to the dissolved pool depending on how mass is distributed among the available fractions. Additional data on particle counts and sizes below 25 μm and on the dissolved fraction would improve model fits. For 1 cm^2 film pieces, the model also shows a strong fit, especially at early data points, and effectively follows the observed pattern of particle number evolution across size bins, with minor discrepancies.

These trends are also evident in the time-evolution plots of particle number concentrations (Fig. 4a+b), which summarize model predictions and experimental data across all timepoints. Here, each size class is represented as a coloured region, with overlaid dots denoting observations. This view confirms the ability of the model to capture the fragmentation pattern over time and highlights when the overall concentration of particles falls below the threshold of 1 particle (>25 μm) per gram of soil. For the cryomilled dataset, this was reached by day 598 (Fig. 4a), and for the 1 cm^2 system by day 686 (Fig. 4b). The threshold of 1 particle per gram of soil (>25 μm) was chosen to represent a concentration below which the model predicts that either no or very few fragments remain. This was chosen over a lower threshold of, for example, 0 particles per gram of soil, because rate-constant-based models such as this tend to trend asymptotically towards 0 without ever reaching it. These results demonstrate the model's ability not only to reproduce observed particle dynamics, but also to provide insight into the timescales over which physical fragmentation effectively concludes in soil environments.

4.3.3. Mass fraction dynamics

The evolution of material mass across particulate, dissolved, and mineralized phases provides further insight into the degradation dynamics of the mulch films. The model tracks how the mass initially present in solid particles shifts progressively into dissolved polymer and eventually into mineralized CO_2 (Fig. 5a+b). In both cryomilled and 1 cm^2 film systems, the model reveals distinct degradation trajectories. For cryomilled fragments and the 1 cm^2 films, a rapid transition is observed: by approximately day 400, the system is almost entirely composed of CO_2, which means that the vast majority of the initial mass has been mineralized. Additionally, the mass fraction, defined as the ratio of a component's mass to the total initial mass, sums to approximately 1 throughout the simulation, confirming near-conservation of mass in the system. This consistency underscores the model's internal validity and ensures that mass transfer processes—fragmentation, dissolution, and mineralization—are properly balanced within the computational framework.

4.3.4. Fragmentation size distribution

To better understand how particles fragment into smaller size classes, the Fragmentation Size Distribution (FSD) for both cryomilled and 1 cm^2 films is analyzed (Fig. 6). Cryomilled films exhibit predominantly cascading mass transfer to the next smaller size class (i.e. particle shrinking): each parent size class nearly entirely transforms into the

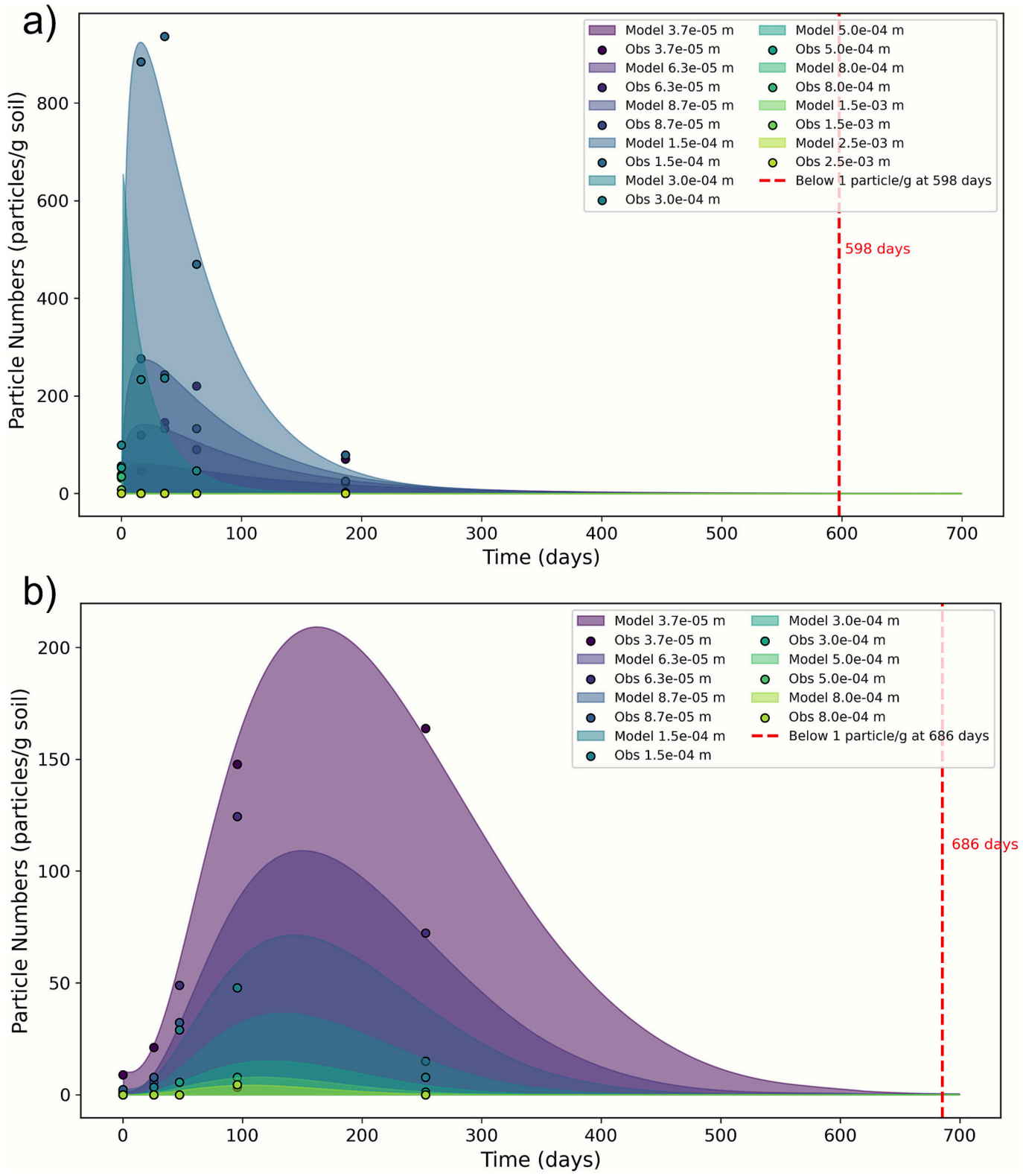

Fig. 4. a) Time evolution of particle number concentrations for the cryomilled mulch film. The stacked area plot shows model predictions for each size class (viridis colour scale). Coloured dots represent observed data. By day 598, the total particle concentration drops below 1 particle per gram of soil; b) Time evolution of particle number concentrations for the 1 cm^2 mulch film. The stacked area plot shows model predictions for each size class (viridis colour scale). Coloured dots represent observed data. By day 686, the total particle concentration drops below 1 particle per gram of soil.

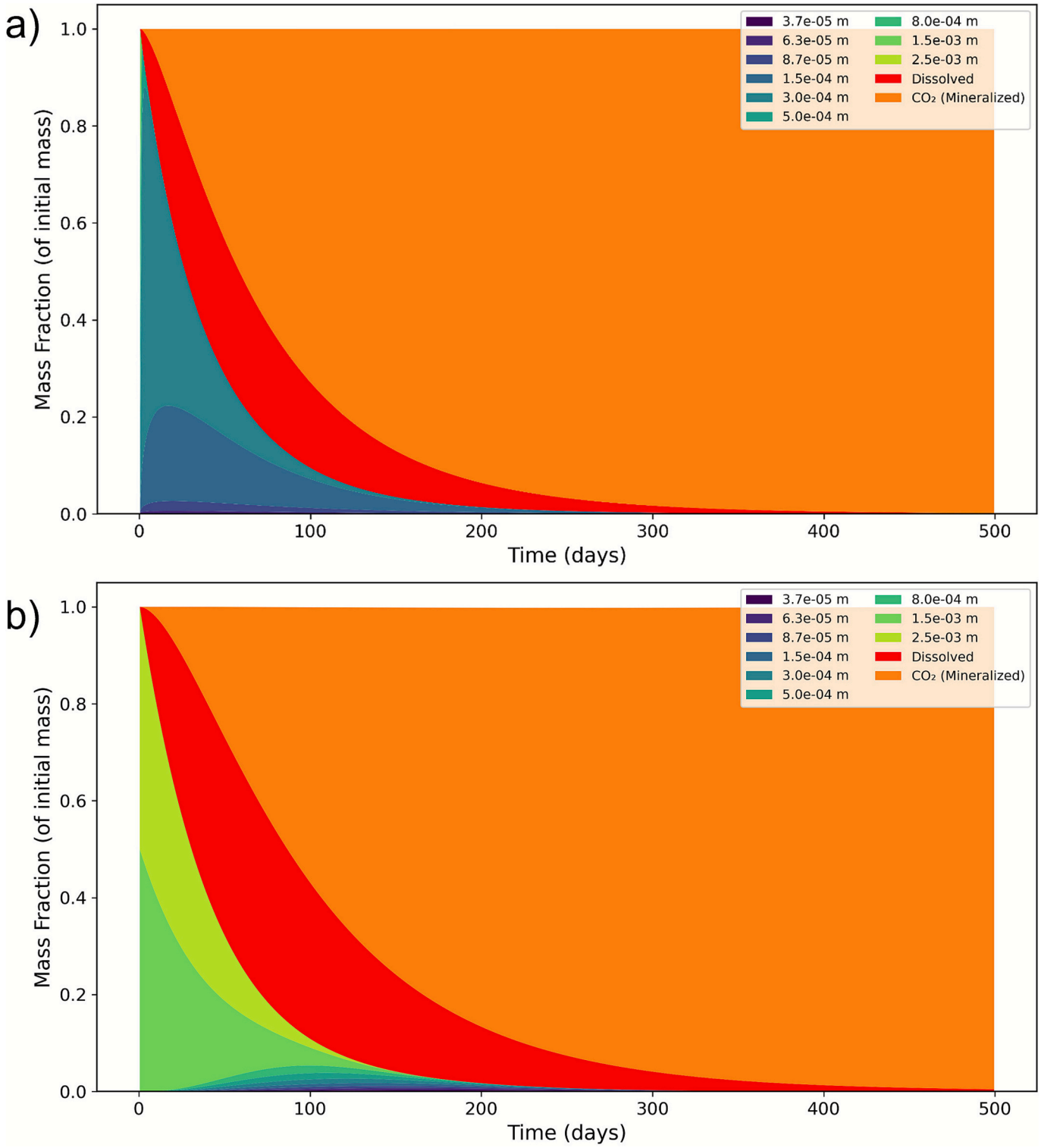

Fig. 5. a) Mass fraction evolution for the cryomilled mulch film. The plot shows the normalized mass of all components (size bins in viridis, dissolved in red, CO_2 in orange); b) Mass fraction evolution for the 1 cm^2 mulch film. The plot shows the normalized mass of all components (size bins in viridis, dissolved in red, CO_2 in orange).

subsequent size class, resulting in bar plots that are largely monochromatic within each column. In contrast, 1 cm^2 films fragment into several size bins of smaller particles: each parent size class produces fragments across multiple smaller size classes, as evidenced by the multicoloured bar patterns (Fig. 6), though about 40 % of the mass still transfers to the next smaller size class. A potential explanation for this could be that the surface erosion on the 1 cm^2 pieces creates localized thinning both by biological inhomogeneity (e.g. hyphae and microbial colonization) and geometric thickness variation (Pfohl et al., 2024a).

5. Conclusion

Overall, the experimental and modelling results clearly demonstrate that biodegradation and fragmentation of the certified soil-

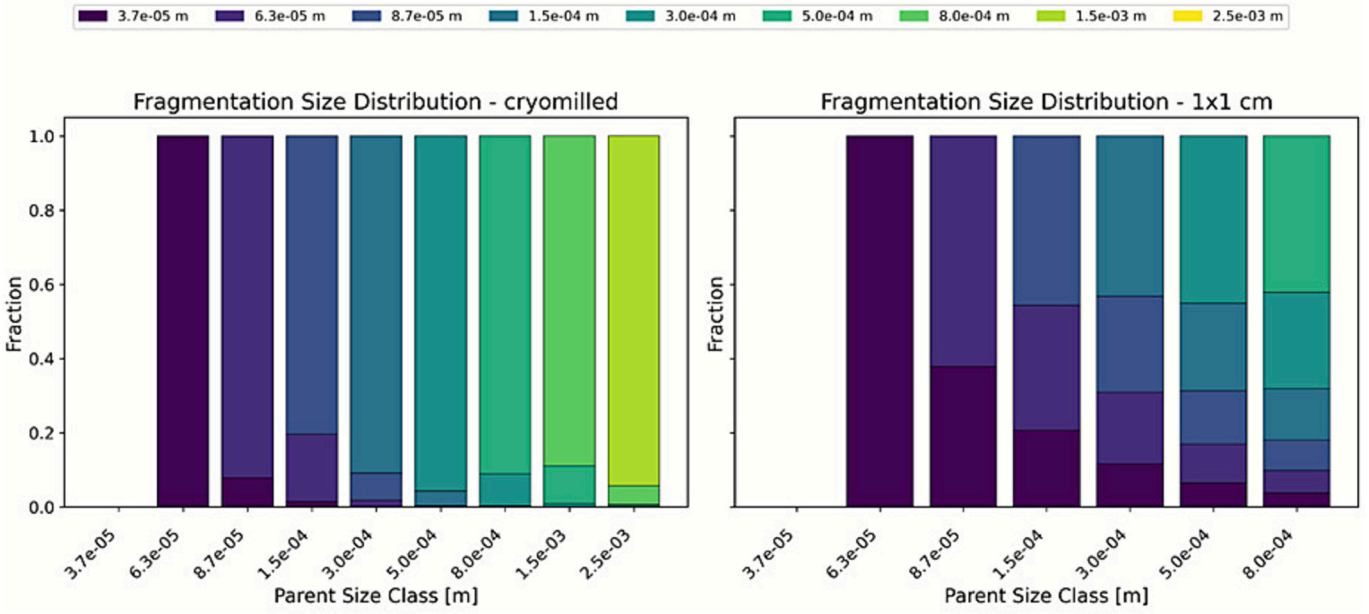

Fig. 6. Fragmentation Size Distribution (FSD) Comparison for cryomilled (left) and 1 cm^2 film pieces (right). Each panel displays a matrix of bar plots showing the fraction of mass distributed into smaller fragment size classes (y-axis) for each parent particle size class (x-axis). In the cryomilled dataset, fragmentation produces primarily a single dominant daughter size, while in the 1 cm^2 dataset, fragmentation leads to a broader distribution across multiple smaller sizes. The colour gradient reflects the contribution of each size class (viridis colourmap).

biodegradable mulch film ecovio® M2351 are interconnected processes, and the transient formation of fragments is part of the biodegradation process. Analytical microscopy techniques, such as μ-FTIR, are capable of measuring the formation and further biodegradation of such fragments, and modelling is able to elucidate the dynamics of this fragment formation and mineralization. As discussed above, a transient increase of fragment counts can occur, even though at the same time the overall mulch film mass is reduced due to polymer biodegradation and mineralization. The biodegradation experiments conducted in this study were performed under controlled and standardized conditions with a high load of polymer per gram soil, not directly reflecting field conditions, but providing insights into the behavior of these materials. Our data also show that the shape of the material influences the biodegradation and fragmentation of the same material. Cryomilled fragments show faster biodegradation, but also stronger fragmentation than larger 1 cm^2 film pieces. Larger film pieces predominantly form fragments <75 μm. Even though the mass of fragments >25 μm was in both cases reduced by more than 98 wt.-%, we still found some fragments at the end of the biodegradation experiment that just had started to biodegrade. Additional analysis revealed the same chemistry (Fig. S8) and even lower molar masses than the original mulch film pieces, also demonstrating that these fragments would have been further mineralized if the biodegradation experiment continued. Experimental data is crucial to understand the ongoing fragmentation processes during biodegradation, but only shows an excerpt of the overall picture, since timepoints for extraction and analysis need to be chosen and results depend on the limit of quantification of the analytical techniques. Additional analytical techniques, such as pyr-GCMS, LCMS, or μ-Raman could be employed in future studies to assess particles <25 μm and to quantify polymer present in the dissolved phase. Still, mechanistic fragmentation and degradation models are needed to translate the lab-scale simulations to the real world (Domercq et al., 2022; Koelmans et al., 2017; Kaandorp et al., 2021; Harrison et al., 2024). Here, we have used modelling to predict how long it takes before there are no or very few fragments (<1 particle per gram of soil), which under these standardized laboratory conditions was around 600–700 days. Furthermore, we can use modelling to evaluate fragmentation peaks and extrapolation for half-live predictions (Wohlleben et al., 2024). Our current results confirm that fragmentation and mineralization for the cryomilled polymer is quicker than for the 1 cm^2 film pieces, showing a fragmentation peak at a much earlier timepoint (Fig. 4), and a shorter period during which polymer is in the dissolved phase (Fig. 5).

Finally, it should be noted that extrapolating the current model predictions to real-world conditions requires accounting for variations in temperature, humidity, microbial diversity, and soil composition in the environment. Biodegradation and fragmentation rates can vary with season and geographic location. The model that is now established can as well be fitted to the fragmentation kinetics measured as time series in field conditions. The overall rates may be slower under certain conditions, e.g. in cold climates, but re-distribution to smaller fragment sizes, to oligomers and ultimately CO_2 would still be the basic mechanism. We therefore encourage further investigations to confirm and extend our findings under a variety of environmental conditions to support the further parameterization of the FRAGMENT-MNP model.

Associated content

The following file is available free of charge: Additional information on technical properties of the mulch film and the soil, detailed biodegradation curves of both campaigns (cryomilled and 1 cm^2 pieces), soil blank data, total particle mass over CO_2, detailed particle size distributions of both campaigns (cryomilled and 1 cm^2 pieces), μ-FTIR spectra of ecovio® M2351 (PDF).

CRediT authorship contribution statement

Patrizia Marie Schmidt: Writing – review & editing, Writing – original draft, Supervision, Project administration, Methodology, Investigation, Data curation, Conceptualization. **Lukas Leibig:** Writing – review & editing, Writing – original draft, Formal analysis. **Lars Meyer:** Writing – review & editing, Writing – original draft, Supervision, Formal analysis, Data curation. **Christian Roth:** Writing – review & editing, Methodology. **Patrick Bolduan:** Writing – review & editing, Supervision, Methodology, Conceptualization. **Glauco Battagliarin:** Writing – review & editing, Writing – original draft, Supervision, Methodology, Investigation, Formal analysis, Conceptualization.

Andreas Künkel: Writing – review & editing, Supervision. **Sam Harrison:** Writing – review & editing, Writing – original draft, Validation, Software, Methodology, Formal analysis, Data curation, Conceptualization. **Cansu Uluseker:** Writing – review & editing, Writing – original draft, Visualization, Validation, Software, Methodology, Formal analysis, Data curation. **Wendel Wohlleben:** Writing – review & editing, Validation, Supervision, Project administration, Methodology, Investigation, Conceptualization.

Funding

This research did not receive any specific grant from funding agencies in the public, commercial, or not-for-profit sectors.

Declaration of competing interest

The authors declare the following financial interests/personal relationships which may be considered as potential competing interests: Some of the authors are employees of BASF SE, a company producing and marketing polymers, including biodegradable polymers.

If there are other authors, they declare that they have no known competing financial interests or personal relationships that could have appeared to influence the work reported in this paper.

Acknowledgments

The authors sincerely thank Bastiaan Staal (GPC) for his scientific advice on molar mass analysis. We would also like to express our sincere gratitude to Afsaneh Nabifar and Dawid Marczewski for their invaluable contributions to the interpretation of the results we obtained.

Appendix A. Supplementary data

Supplementary data to this article can be found online at https://doi.org/10.1016/j.scitotenv.2025.181048.

Data availability

All data generated or analyzed during this study are included in this published article and its supplementary information files.

References

Araujo, C.F., Nolasco, M.M., Ribeiro, A.M.P., Ribeiro-Claro, P.J.A., 2018. Identification of microplastics using Raman spectroscopy: latest developments and future prospects. Water Res. 142, 426–440. https://doi.org/10.1016/j.watres.2018.05.060.

Binda, G., Kalčíková, G., Allan, I.J., Hurley, R., Rødland, E., Spanu, D., Nizzetto, L., 2024. Microplastic aging processes: environmental relevance and analytical implications. TrAC Trends Anal. Chem. 172. https://doi.org/10.1016/j.trac.2024.117566.

BASF SE, 2024. ecovio® M2351-Biodegradable Compound for Agricultural Film. BASF SE. Product Information 1.0.

Brouwer, M.T., Post, W., van der Zee, M., Reilink, R., Boom, R., Maaskant, E., 2024. A predictive model to assess the accumulation of microplastics in the natural environment. Sci. Total Environ. 957, 177503. https://doi.org/10.1016/j.scitotenv.2024.177503.

Chen, L., Imam, S.H., Gordon, S.H., Greene, R.V., 1997. Starch-polyvinyl alcohol crosslinked film - performance and biodegradation. Journal of Environmental Polymer Degradation 5, 111–117.

Chen, M., Coleman, B., Gaburici, L., Prezgot, D., Jakubek, Z.J., Sivarajah, B., Vermaire, J. C., Lapen, D.R., Velicogna, J.R., Princz, J.I., Provencher, J.F., Zou, S., 2024. Identification of microplastics extracted from field soils amended with municipal biosolids. Sci. Total Environ. 907, 168007. https://doi.org/10.1016/j.scitotenv.2023.168007.

Chinaglia, S., Tosin, M., Degli-Innocenti, F., 2018. Biodegradation rate of biodegradable plastics at molecular level. Polym. Degrad. Stab. 147, 237–244. https://doi.org/10.1016/j.polymdegradstab. 2017.12.011.

Degli-Innocenti, F., 2024. The pathology of hype, hyperbole and publication bias is creating an unwarranted concern towards biodegradable mulch films. J. Hazard. Mater. 463, 132923. https://doi.org/10.1016/j.jhazmat.2023.132923.

Domercq, P., Praetorius, A., MacLeod, M., 2022. The full multi: an open-source framework for modelling the transport and fate of nano- and microplastics in aquatic systems. Environ. Model. Software 148, 105291. https://doi.org/10.1016/j.envsoft.2021.105291.

ECHA, 2019. Annex XV Restriction Report: Microplastics. https://echa.europa.eu/documents/10162/827ab66d-8f59-9076-e000-064274ba5b5e.

Erlandsson, B., Karlsson, S., Albertsson, A.C., 1998. Correlation between molar mass changes and CO2 evolution from biodegraded14C-labeled ethylene-vinyl alcohol copolymer and ethylene polymers. Acta Polym. 49, 363–370. https://doi.org/10.1002/(sici)1521-4044(199807)49:7<363::Aid-apol363>3.0.Co;2-u.

European Commission, 2024. Ecodesign for Sustainable Products Regulation. https://commission.europa.eu/energy-climate-change-environment/standards-tools-and-labels/products-labelling-rules-and-requirements/ecodesign-sustainable-products-regulation_en. (Accessed 10 September 2024).

Gao, X., Xie, D., Yang, C., 2021. Effects of a PLA/PBAT biodegradable film mulch as a replacement of polyethylene film and their residues on crop and soil environment. Agric Water Manag 255. https://doi.org/10.1016/j.agwat.2021.107053.

Gu, X., Cai, H., Fang, H., Chen, P., Li, Y., Li, Y., 2021. Soil hydro-thermal characteristics, maize yield and water use efficiency as affected by different biodegradable film mulching patterns in a rain-fed semi-arid area of China. Agric Water Manag 245. https://doi.org/10.1016/j.agwat.2020.106560.

Harrison, S., Lopez, B., Wiesner, M., 2024. FRAGMENT-MNP [Computer software]. https://github.com/microplastics-cluster/fragment-mnp.

Harrison, S., Uluseker, C., Pfohl, P., Santizo, K., Sipe, J., Lopez, B., Praetorius, A., Cross, R.K., Adediran, G.A., Svendsen, C., Wohlleben, W., Wiesner, M., 2025. FRAGMENT-MNP: a model of micro- and nanoplastic fragmentation in the environment. The Journal of Open Source Software 10 (110), 8061.

Hofmann, T., Ghoshal, S., Tufenkji, N., Adamowski, J.F., Bayen, S., Chen, Q., Demokritou, P., Flury, M., Hüffer, T., Ivleva, N.P., Ji, R., Leask, R.L., Maric, M., Mitrano, D.M., Sander, M., Pahl, S., Rillig, M.C., Walker, T.R., White, J.C., Wilkinson, K.J., 2023. Plastics can be used more sustainably in agriculture. Commun. Earth Environ. 4. https://doi.org/10.1038/s43247-023-00982-4.

Ivleva, N.P., 2021. Chemical analysis of microplastics and nanoplastics: challenges, advanced methods, and perspectives. Chem. Rev. 121, 11886–11936. https://doi.org/10.1021/acs.chemrev.1c00178.

Kaandorp, M.L.A., Dijkstra, H.A., van Sebille, E., 2021. Modelling size distributions of marine plastics under the influence of continuous cascading fragmentation. Environ. Res. Lett. 16. https://doi.org/10.1088/1748-9326/abe9ea.

Kappler, A., Fischer, D., Oberbeckmann, S., Schernewski, G., Labrenz, M., Eichhorn, K.J., Voit, B., 2016. Analysis of environmental microplastics by vibrational microspectroscopy: FTIR, Raman or both? Anal. Bioanal. Chem. 408, 8377–8391. https://doi.org/10.1007/s00216-016-9956-3.

Koelmans, A.A., Kooi, M., Law, K.L., van Sebille, E., 2017. All is not lost: deriving a top-down mass budget of plastic at sea. Environ. Res. Lett. 12. https://doi.org/10.1088/1748-9326/aa9500.

Künkel, A., Becker, J., Börger, L., Hamprecht, J., Koltzenburg, S., Loos, R., Schick, M.B., Schlegel, K., Sinkel, C., Skupin, G., Yamamoto, M., 2016. Polymers, Biodegradable. In: Ullman's Encyclopedia of Industrial Chemistry. Wiley, pp. 1–29.

Leja, K., Lewandowicz, G., 2010. Polymer biodegradation and biodegradable polymers - a review. Pol. J. Environ. Stud. 19, 255–266.

Li, N.Y., Qu, J.H., Yang, J.Y., 2023a. Microplastics distribution and microbial community characteristics of farmland soil under different mulch methods. J. Hazard. Mater. 445, 130408. https://doi.org/10.1016/j.jhazmat.2022.130408.

Li, P., Lai, Y., Zheng, R.G., Li, Q.C., Sheng, X., Yu, S., Hao, Z., Cai, Y.Q., Liu, J., 2023b. Extraction of common small microplastics and nanoplastics embedded in environmental solid matrices by tetramethylammonium hydroxide digestion and dichloromethane dissolution for Py-GC-MS determination. Environ. Sci. Technol. 57, 12010–12018. https://doi.org/10.1021/acs.est.3c03255.

Liu, E.K., He, W.Q., Yan, C.R., 2014. 'White revolution' to 'white pollution'—agricultural plastic film mulch in China. Environ. Res. Lett. 9, 091001.

Merino, D., Mansilla, A.Y., Casalongué, C.A., Alvarez, V.A., 2019. Polymers for Agri-Food Applications. Ch. Chapter 12, pp. 215–240.

Möller, J.N., Heisel, I., Satzger, A., Vizsolyi, E.C., Oster, S.D.J., Agarwal, S., Laforsch, C., Löder, M.G.J., 2022. Tackling the challenge of extracting microplastics from soils: a protocol to purify soil samples for spectroscopic analysis. Environ. Toxicol. Chem. 41, 844–857. https://doi.org/10.1002/etc.5024.

Nelson, T.F., Remke, S.C., Kohler, H.-P.E., McNeill, K., Sander, M., 2020. Quantification of synthetic polyesters from biodegradable mulch films in soils. Environ. Sci. Technol. 54, 266–275.

Okoffo, E.D., Thomas, K.V., 2024. Quantitative analysis of nanoplastics in environmental and potable waters by pyrolysis-gas chromatography-mass spectrometry. J. Hazard. Mater. 464, 133013. https://doi.org/10.1016/j.jhazmat.2023.133013.

Park, S.Y., Kim, C.G., 2022. A comparative study on the distribution behavior of microplastics through FT-IR analysis on different land uses in agricultural soils. Environ. Res. 215, 114404. https://doi.org/10.1016/j.envres.2022.114404.

Pfohl, P., Bahl, D., Rückel, M., Wagner, M., Meyer, L., Bolduan, P., Battagliarin, G., Hüffer, T., Zumstein, M., Hofmann, T., Wohlleben, W., 2022. Effect of polymer properties on the biodegradation of polyurethane microplastics. Environ. Sci. Technol. 56, 16873–16884. https://doi.org/10.1021/acs.est.2c05602.

Pfohl, P., Rueckel, M., Meyer, L., Battagliarin, G., Künkel, A., Hüffer, T., Zumstein, M., Hofmann, T., Wohlleben, W., 2024a. Influence of plastic shape on interim fragmentation of compostable materials during composting. Microplastics and Nanoplastics 4. https://doi.org/10.1186/s43591-024-00084-8.

Pfohl, P., Roth, C., Wohlleben, W., 2024b. The power of centrifugation: how to extract microplastics from soil with high recovery and matrix removal efficiency. MethodsX 12. https://doi.org/10.1016/j.mex.2024.102598.

Rillig, M.C., Ingraffia, R., de Souza Machado, A.A., 2017. Microplastic incorporation into soil in agroecosystems. Front. Plant Sci. 8, 1805. https://doi.org/10.3389/fpls.2017.01805.

Ruffell, H., Pantos, O., Robinson, B., Gaw, S., 2024. A method for the extraction of microplastics from solid biowastes including biosolids, compost, and soil for analysis by micro-FTIR. MethodsX 12, 102761. https://doi.org/10.1016/j.mex.2024.102761.

Sander, M., 2019. Biodegradation of polymeric mulch films in agricultural soils: concepts, knowledge gaps, and future research directions. Environ. Sci. Technol. 53, 2304–2315. https://doi.org/10.1021/acs.est.8b05208.

Schwaferts, C., Sogne, V., Welz, R., Meier, F., Klein, T., Niessner, R., Elsner, M., Ivleva, N. P., 2020. Nanoplastic analysis by online coupling of Raman microscopy and field-flow fractionation enabled by optical tweezers. Anal. Chem. 92, 5813–5820. https://doi.org/10.1021/acs.analchem.9b05336.

Su, X., Liu, M., Dou, J., Yuan, J., Cheng, J., Lu, Z., He, Y., 2024. A review on enriched microplastics in environment: from the perspective of their aging impact and associate risk. Earth Critical Zone 1. https://doi.org/10.1016/j.ecz.2024.100008.

Uluseker, C., Schmidt, P., Harrison, S., Wohlleben, W., 2025. Fragment-MNP mulch film optimization: soil-biodegradable mulch film: distinguishing between persistent microplastics and fragments released from certified soil-biodegradable products. Zenodo. https://doi.org/10.5281/zenodo.15535827.

von Vacano, B., Mangold, H., Vandermeulen, G.W.M., Battagliarin, G., Hofmann, M., Bean, J., Kunkel, A., 2022. Sustainable design of structural and functional polymers for a circular economy. Angew. Chem. Int. Ed. Engl. 62, e2022108. https://doi.org/10.1002/anie.202210823.

Wang, T., Ma, Y., Ji, R., 2021. Aging processes of polyethylene mulch films and preparation of microplastics with environmental characteristics. Bull. Environ. Contam. Toxicol. 107, 736–740. https://doi.org/10.1007/s00128-020-02975-x.

Wohlleben, W., Rückel, M., Meyer, L., Pfohl, P., Battagliarin, G., Hüffer, T., Zumstein, M. T., Hofmann, T., 2023. Fragmentation and mineralization of a compostable aromatic-aliphatic polyester during industrial composting. Environ. Sci. Technol. Lett. 10, 698–704. https://doi.org/10.1021/acs.estlett.3c00394.

Wohlleben, W., Bossa, N., Mitrano, D.M., Scott, K., 2024. Everything falls apart: how solids degrade and release nanomaterials, composite fragments, and microplastics. NanoImpact 34, 100510. https://doi.org/10.1016/j.impact.2024.100510.

Żenkiewicz, M., Malinowski, R., Rytlewski, P., Richert, A., Sikorska, W., Krasowska, K., 2012. Some composting and biodegradation effects of physically or chemically crosslinked poly(lactic acid). Polym. Test. 31, 83–92. https://doi.org/10.1016/j.polymertesting.2011.09.012.

Zhang, C., Liu, X., Zhang, L., Chen, Q., Xu, Q., 2024. Assessing the aging and environmental implications of polyethylene mulch films in agricultural land. Environ. Sci. Process Impacts 26, 1310–1321. https://doi.org/10.1039/d4em00102h.

Zumstein, M.T., Schintlmeister, A., Nelson, T.F., Baumgartner, R., Woebken, D., Wagner, M., Kohler, H.-P.E., McNeill, K., Sander, M., 2018. Biodegradation of synthetic polymers in soils: tracking carbon into CO2 and microbial biomass. Sci. Adv. 4, 1–8.